

## Effect of Resonant and Non-resonant Magnetic Braking on Error Field Tolerance in High Beta Plasmas

H. Reimerdes 1), A.M. Garofalo 2), E.J. Strait 2), R.J. Buttery 3), M.S. Chu 2), Y. In 4), G.L. Jackson 2), R.J. La Haye 2), M.J. Lanctot 1), Y.Q. Liu 3), J.-K. Park 5), M. Okabayashi 5), M.J. Schaffer 2), and W.M. Solomon 5)

1) Columbia University, New York, New York 10027, USA

2) General Atomics, P.O. Box 85608, San Diego, California 92186-5608, USA

3) EURATOM/UKAEA Fusion Association, Culham Science Centre, OX14 3DB, UK

4) FAR-TECH, Inc., San Diego, California 92121, USA

5) Princeton Plasma Physics Laboratory, Princeton, New Jersey 08543-0451, USA

e-mail contact of main author: reimerdes@fusion.gat.com

**Abstract.** Tokamak plasmas become less tolerant to externally applied non-axisymmetric magnetic “error” fields as beta increases, due to a resonant interaction of the non-axisymmetric field with a stable  $n=1$  kink mode. Similar to observations in low beta plasmas, the limit to tolerable  $n=1$  magnetic field errors in neutral beam injection heated H-mode plasmas is seen as a bifurcation in the torque balance, which is followed by error field driven locked modes and severe confinement degradation or a disruption. The error field tolerance is, therefore, largely determined by the braking torque resulting from the non-axisymmetric magnetic field. DIII-D experiments distinguish between a resonant-like torque, which decreases with increasing rotation, and a non-resonant-like torque, which increases with increasing rotation. While only resonant braking leads to a rotation collapse, modeling shows that non-resonant components can lower the tolerance to resonant components. The strong reduction of the error field tolerance with increasing beta, which has already been observed in early high beta experiments in DIII-D [R.J. La Haye, et al., Nucl. Fusion **32**, 2119 (1992)], is linked to an increasing resonant field amplification resulting from a stable kink mode [A.H. Boozer, Phys. Rev. Lett. **86**, 5059 (2001)]. The amplification of externally applied  $n=1$  fields is measured with magnetic pick-up coils and seen to increase with beta, with the increase accelerating above the no wall ideal MHD stability limit, where the ideal MHD stable kink mode converts to a kinetically stabilized resistive wall mode. The beta dependence was not previously appreciated, and was not included in the empirical scaling of the error field tolerance reported in the 1999 IPB [ITER Physics Basis, Nucl. Fusion **39**, 2137 (1999)] leading to overly optimistic predictions for low torque, high beta scenarios. However, the measurable increase of the plasma response with beta can be exploited for “dynamic” correction (i.e. with slow magnetic feedback) of the amplified error field.

### 1. Introduction

Tokamak plasmas are very sensitive to non-axisymmetric perturbations of the externally applied magnetic “error” field. Small perturbations in the order of  $\delta B^{\text{ext}}/B_T \approx 10^{-4}$ , where  $B_T$  is the toroidal magnetic field, can lead to locked modes in Ohmically heated, low density plasmas and to rotation and pressure collapses in neutral beam injection (NBI) heated H-mode discharges. While the error field tolerance is usually described by empirical scaling laws (e.g., [1]), which are based on Ohmic locked mode experiments (e.g., [2]) and mainly depend on the electron density  $n_e$ , early high  $\beta$  experiments in DIII-D, with  $\beta \equiv 2\mu_0 \langle p \rangle / B_T^2$  being the normalized volume averaged plasma pressure, already showed a strong reduction of the error field tolerance with  $\beta$  [3]. The  $n=1$  error field threshold in high  $\beta$  discharges was initially interpreted as a stability threshold with magnetic braking leading to a loss of rotational stabilization and, consequently, an unstable resistive wall mode (RWM). However, it has recently been pointed out that, similar to the low  $\beta$  locked mode experiments, the  $n=1$  error field tolerance of high  $\beta$  plasmas is caused by a bifurcation in the torque balance [4]. The presented work investigates the role of magnetic braking in determining the error field tolerance of high  $\beta$  plasmas, draws the link to low  $\beta$  experiments and discusses the consequences for ITER.

## 2. Error Field Tolerance of High Beta Plasmas

The error field tolerance is systematically studied in controlled magnetic braking experiments in weakly shaped, lower-single null H-mode discharges ( $B_T = 2.0$  T,  $I_p = 1.1$  MA,  $q_{95} \approx 4.9$ ,  $q_{\min} \approx 1.5$ ), which have Advanced Tokamak relevant  $q$ -profiles but low ideal MHD  $\beta$  limits. The experiments take advantage of the flexible non-axisymmetric control coil sets on DIII-D. While a set of six external control coils (C-coils) empirically corrects the intrinsic error field, two sets of six internal control coils each (I-coils) located above and below the outboard midplane apply a well-known non-axisymmetric perturbation. The phase difference  $\Delta\phi_I$  between the  $n = 1$  field applied with the upper and the lower I-coil arrays can be varied to modify the poloidal spectrum of the externally applied field. The I-coil is usually configured with a phase difference  $\Delta\phi_I = 240$  deg, where 1 kA of  $n = 1$  current generates a resonant field at the  $q = 2$  surface of approximately  $B_{21}^{\text{ext}} \approx 1.0$  G.

### 2.1. Torque Balance and Error Field Penetration

In order to study the torque balance, the I-coil currents are programmed to generate a slowly rotating (10 Hz)  $n = 1$  field whose amplitude increases on a time scale, which is slow compared to a typical angular momentum confinement time  $\tau_L$  of 50 ms, Fig. 1(a,b). As the  $n = 1$  field is ramped up, the toroidal plasma rotation  $\Omega$ , which is measured with charge exchange recombination spectroscopy using C-VI emission, decreases, Fig. 1(c), and the  $n = 1$  plasma response  $B_p^{\text{plas}}$ , measured with a toroidal array of poloidal magnetic field probes at the outboard midplane increases, Fig. 1(d), until the rotation collapses at  $t = 2910$  ms. The collapse is followed by an error field-driven locked mode, which can be seen on the electron temperature  $T_e$  contours Fig. 1(e) as the externally applied field rotates the island past the electron cyclotron emission (ECE) diagnostic [5] and which leads to a severe degradation of the confinement. The characteristics of the error field limit in these high  $\beta$  H-modes are similar to the observations in low density, locked mode experiments in Ohmic plasmas (e.g., [2]). It is understood that a sufficiently large plasma rotation induces helical currents at rational surfaces  $q = m/n$ , which cancel the resonant harmonics of the externally applied field and suppress the formation of islands. The finite resistivity leads to dissipation and consequently a torque, which slows the plasma rotation. The evolution of the plasma rotation can be described by

$$I \frac{d\Omega}{dt} = T_{\text{in}} - \frac{I\Omega}{\tau_{L,0}} - T_{\text{MB}} \quad , \quad (1)$$

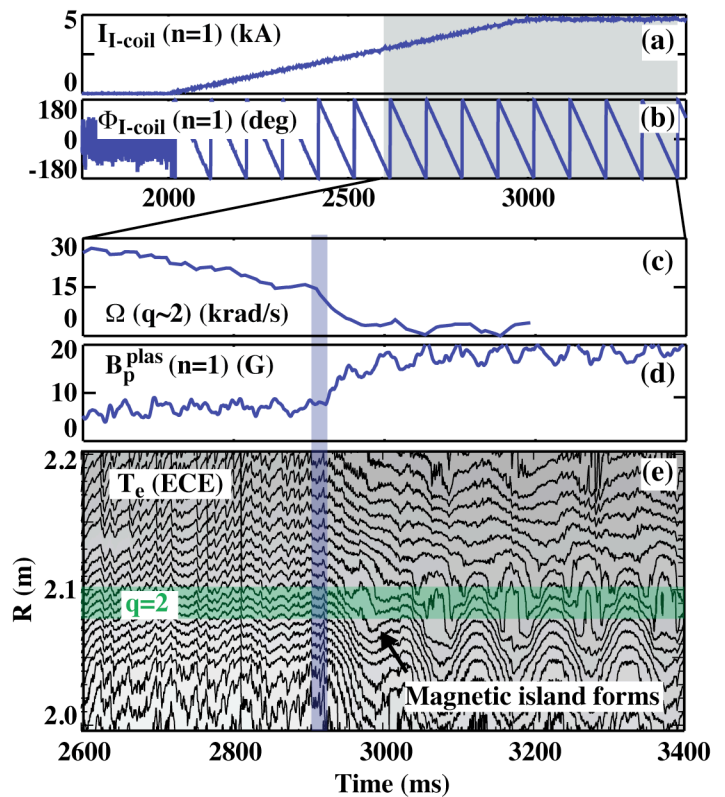


FIG. 1. Increasing the amplitude of a slowly rotating  $n = 1$  I-coil field (a,b) leads to a decrease of the rotation  $\Omega$  (c) and an increase of the  $n = 1$  plasma response  $B_p^{\text{plas}}$  (d). The rotation collapse is followed by “error” field penetration seen on the electron temperature  $T_e$  contours (e).

where  $I$  is the moment of inertia,  $T_{\text{in}}$  the sum of all accelerating torques and  $\tau_{L,0}$  the momentum confinement time in the absence of non-axisymmetric fields. When the magnetic braking torque  $T_{\text{MB}}$  increases sufficiently fast with decreasing  $\Omega$ , the torque balance can be lost and the rotation collapses [6]. If  $T_{\text{MB}}$  is proportional to  $\Omega^{-1}$  and the viscous transport described by a momentum confinement time, the torque balance Eq. (1) predicts this bifurcation to occur at a critical rotation  $\Omega_{\text{crit}} = T_{\text{in}}\tau_{L,0}/(2I)$ . If  $T_{\text{in}}$  is kept constant, this corresponds to half of the unperturbed rotation,  $\Omega_{\text{crit}} = \Omega_0/2$ . When the plasma rotation is too low to induce the helical shielding currents, the error field penetrates and an island opens, consistent with the observations, Fig. 1. In DIII-D the characteristic relation between  $\Omega_0$  and  $\Omega_{\text{crit}}$  has been observed in several plasma scenarios and over a wide range of rotation values [4,7].

High  $\beta$  low rotation discharges are also particularly prone to the onset of  $m/n=2/1$  neoclassical tearing modes (NTMs) [8] caused by a decrease of their  $\beta_N$  threshold with decreasing rotation in the direction of the plasma current [9]. In addition to affecting the tearing stability through braking of the plasma rotation, non-axisymmetric fields are also thought to directly reduce the NTM  $\beta_N$  threshold [10]. These modes, which are typically born rotating but quickly lock, are occasionally observed during the I-coil ramps and limit operation towards higher  $\beta_N$  and lower  $\Omega$ .

## 2.2. Torque Balance and Dependence of Error Field Tolerance on NBI Torque/Rotation

Since the error field tolerance is determined by the loss of torque balance, it should improve with increasing torque input to the plasma. Assuming a visco-resistive resonant magnetic braking torque,  $T_{\text{MB}} = K_R \delta B_R^2 \Omega^{-1}$  [6], the torque balance according to Eq. (1) is lost when the magnetic perturbation exceeds a critical amplitude,

$$\delta B_{R,\text{crit}} = T_{\text{in}} \left( \frac{\tau_{L,0}}{4 I K_R} \right)^{1/2}. \quad (2)$$

According to Eq. (2), the error field tolerance should increase linearly with the NBI torque  $T_{\text{NBI}}$ , which is usually the dominant torque input.

The dependence of the  $n = 1$  error field tolerance on  $T_{\text{NBI}}$  is measured using the DIII-D capability to vary  $T_{\text{NBI}}$  independently of the NBI heating power  $P_{\text{NBI}}$ . The externally applied  $n = 1$  field is increased in discharges, which only differ in the value of  $T_{\text{NBI}}$ . In these discharges feedback control of  $P_{\text{NBI}}$  keeps  $\beta_N = 2.0$  constant. Varying  $T_{\text{NBI}}$  by a factor of 3 leads to an increase of the tolerable I-coil current  $I_{\text{crit}}$ , and hence the tolerable externally applied field, by 50%, Fig. 2. Comparing a linear fit of  $I_{\text{crit}}$  versus  $T_{\text{NBI}}$  with Eq. (2) yields a torque offset  $T_0 = T_{\text{in}} - T_{\text{NBI}}$  of 7Nm. While such an offset in the direction of the plasma current could be due to the intrinsic rotation of the plasma, a value of 7Nm is several times larger than expected [11]. Alternatively, the increase of error field tolerance with increasing  $T_{\text{NBI}}$  could be reduced due to a deviation from the  $\Omega^{-1}$  dependence of  $T_{\text{MB}}$  as discussed in Section 3.3.

## 2.3. Dependence of Error Field Tolerance on Beta and Role of Plasma Response

The dependence of the  $n = 1$  error field tolerance on  $\beta_N$  is measured in similar discharges with  $\beta_N$  ranging from 1.5 to 2.3. A comparison of two discharges with  $T_{\text{NBI}} = 1.8$  Nm shows that a 33% increase in  $\beta_N$  from 1.5 and 2.0, Fig. 3(a), halves the tolerable externally applied field ( $\propto I_{\text{crit}}$ ), Fig. 3(b). At higher  $\beta_N$  a smaller externally applied field leads to a similar rotation decay and the rotation collapse occurs at approximately the same rotation, Fig. 3(c).

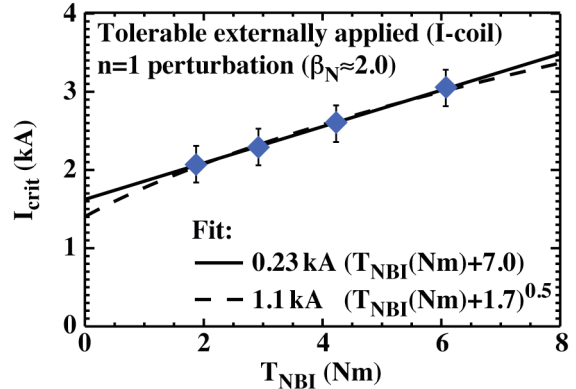


FIG. 2. The tolerable  $n = 1$  I-coil field ( $\propto I_{\text{crit}}$ ) increases with increasing NBI torque  $T_{\text{NBI}}$ . A linear fit yields a torque offset of 7.0 Nm. An alternative fit is discussed in Section 3.3.

At higher  $\beta_N$  the  $n = 1$  plasma response  $B_p^{\text{plas}}$  to the externally applied field is, however, also larger resulting in the same  $B_p^{\text{plas}}$  at the time of the rotation collapse, Fig. 3(d). The continuation of the  $\beta_N$  scan at a higher value of  $T_{\text{NBI}} \approx 4.2$  Nm shows that the decrease of the error field tolerance  $\beta_N$  with  $\beta_N$  even accelerates at higher values of  $\beta_N$ , Fig. 3(e). Again the plasma response to the externally applied field increases accordingly so that  $B_p^{\text{plas}}$  at the collapse remains constant, Fig. 3(f). The observed  $\beta_N$  dependence of the tolerance to externally applied  $n = 1$  fields can, therefore, be explained by a magnetic braking torque that dominantly depends on the plasma response rather than the externally applied (vacuum) perturbation. The tolerable plasma perturbation  $B_{p,\text{crit}}^{\text{plas}}$  increases with  $T_{\text{NBI}}$ , consistent with the results of the torque scan in Section 2.2.

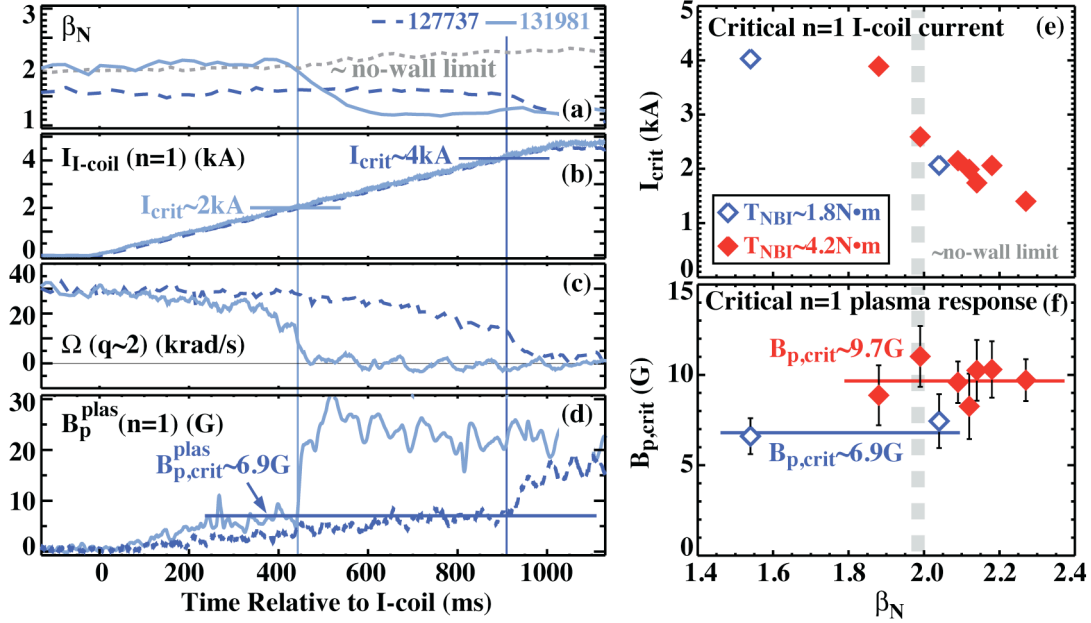


FIG. 3. At constant  $T_{\text{NBI}} \approx 1.8$  Nm the discharge with the higher  $\beta_N$  (a) displays a lower tolerance against  $n = 1$  field asymmetries applied with the I-coil (b) than the discharge with a lower  $\beta_N$ . The collapse of the rotation  $\Omega$  (c) occurs at the same plasma response  $B_p^{\text{plas}}$  (d). A  $\beta_N$  scan at  $T_{\text{NBI}} \approx 4.2$  Nm (red) (e) shows that the decrease of the tolerance to externally applied  $n = 1$  fields ( $\propto I_{\text{crit}}$ ) with  $\beta_N$  accelerates further when  $\beta_N$  exceeds the no-wall limit. For each value of  $T_{\text{NBI}}$  the plasma response at the collapse  $B_{p,\text{crit}}^{\text{plas}}$  (f) is independent of  $\beta_N$ .

## 2.4. Dependence of the Error Field Tolerance on the Poloidal Spectrum

The dependence of the error field on the poloidal spectrum of the externally applied field is investigated by probing similar plasmas ( $\beta_N \approx 2.2$ ,  $T_{\text{NBI}} = 4.5$  Nm) with I-coil fields that differ from the standard phase difference of  $\Delta\phi_I = 240$  deg, Fig. 4(a). Reducing  $\Delta\phi_I$  to 180 deg allows approximately for a doubling of the I-coil current and, hence, the externally applied field before the rotation collapses, Fig. 4(a,b). In the case of  $\Delta\phi_I = 120$  deg the currents in the I-coil can even be ramped up to the power-supply limited maximum current of 4.5 kA while causing only modest braking. Again the braking is related to the plasma response, with the rotation collapse occurring at  $B_{p,\text{crit}}^{\text{plas}} \approx 10$  G, Fig. 4(c). The coupling of a field resulting from  $\Delta\phi_I = 240$  deg to the plasma is approximately six times more effective than the coupling to a field resulting from  $\Delta\phi_I = 120$  deg, Fig. 4(d). At the same time the resonant component of the externally applied field at the  $q=2$  surface  $B_{21}^{\text{ext}}$  remains the same.

## 2.5. Understanding of the Plasma Response

The role of the plasma response to enhance the torque of uncorrected error fields in wall-stabilized plasmas is well known [12] and has been attributed to resonant amplification of the

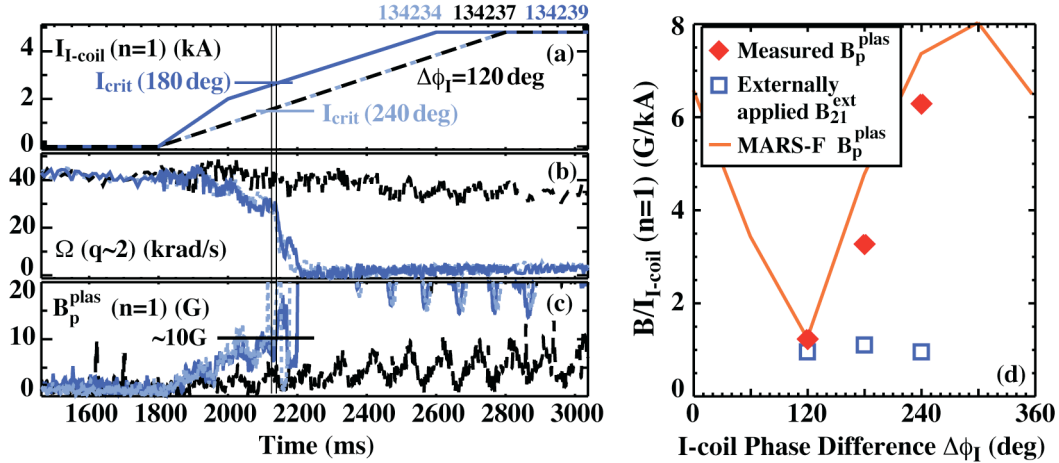


FIG. 4. Discharges with constant  $\beta_N = 2.2$  are perturbed with I-coil fields with different phase differences  $\Delta\phi_I$  (a). While the discharges with  $\Delta\phi_I = 180$  deg and 240 deg experience a rotation collapse (b), the current for  $\Delta\phi_I = 120$  deg can be increased to 4.5 kA while causing only modest braking. The critical current for  $\Delta\phi_I = 180$  deg is higher than for 240 deg, but the corresponding plasma response remains the same (c). While the  $\Delta\phi_I$  dependence of the coupling of the externally applied field to the plasma  $B_p^{\text{plas}}/I_{I\text{-coil}}$  (diamonds) does not correlate with  $B_{21}^{\text{ext}}(q=2)$  (squares), it is well described by modeling with the MARS-F code (d).

weakly damped, but stable  $n = 1$  RWM [13]. Once  $\beta_N$  exceeds the no-wall limit, small externally applied  $n = 1$  fields can drive the stable RWM to a large amplitude.

The interaction of non-axisymmetric fields with the plasma can be modeled with the MARS-F code [14]. It is thought that the stabilization of the RWM is a result of kinetic effects [15], but the present implementation of semi-kinetic stabilization in MARS-F [16] still falls short of a quantitative description of the experimental observations [7]. While a quantitative prediction of the damping rate and, hence amplification is not expected, the code can describe the coupling of external fields to the kink mode. The  $n = 1$  plasma response at the location of the  $B_p$  measurements is calculated for I-coil fields with various phase differences  $\Delta\phi_I$ , Fig. 4. The equilibrium of discharge 134234 at  $t = 1750$  ms is ideal MHD unstable and soundwave damping [17] is added to stabilize the plasma. Varying only  $\Delta\phi_I$  yields the best coupling for  $\Delta\phi_I = 300$  deg. The calculation correctly describes the observed large increase of the coupling when  $\Delta\phi_I$  is increased from 120 to 240 deg, Fig. 4(d). It is important to note that the plasma response is not caused by the components of the externally applied field that are resonant with field lines inside the plasma, but by the component with a smaller pitch angle that is “resonant” with the kink mode. The plasma response below the no-wall limit has similar characteristics, showing the same perturbed field pattern at the wall and no evidence for island formation provided the plasma is rotating. It is, therefore, also likely linked to the (ideal MHD stable)  $n = 1$  kink mode.

Error field correction experiments on DIII-D and NSTX have revealed the importance of the ideal MHD plasma response even in Ohmically heated low  $\beta$  plasmas [18]. The present experiments confirm the role of the plasma response at intermediate values of  $\beta_N$ , bridging the gap between locked mode experiments in Ohmic discharges and error-field correction in wall-stabilized high  $\beta_N$  plasmas. Despite a value of  $\beta_N = 1.5$ , which is significantly below the no-wall limit, the plasma response in discharge 127737, Fig. 3(a–d), reaches values of up to  $B_p^{\text{plas}}(n=1) \approx 7$  G prior to the rotation collapse. Modeling of the perturbed field at the rotation collapse using the Ideal Perturbed Equilibrium Code (IPEC) [19] results in a total resonant field at the  $q = 2$  surface of  $B_{21} \approx 52$  G (using PEST coordinates). With an average electron density of  $\langle n_e \rangle = 3.8 \cdot 10^{19} \text{ m}^{-3}$  this value for  $B_{21}$  lines up remarkably well with an extrapolation based on the usual density dependence of the error field tolerance in Ohmic plasmas (e.g., [3]) and the corresponding IPEC calculation for DIII-D [18], which results in  $B_{21} \approx 46$  G. The excess of approximately 15% in 127737 over the Ohmic scaling can easily be

attributed to the modest NBI torque of 1.8 Nm, which should increase the error field tolerance, Section 2.2.

In high  $\beta_N$  discharges experimental observations [20] as well as modeling with the MARS-F code [21] indicate that the response of a stable plasma to externally applied non-axisymmetric fields is well described by a single least stable mode. A similar conclusion is reached from the IPEC analysis of low beta plasmas [18]. Consequently, correction coils even with a poorly matched magnetic field pattern should be effective in suppressing the plasma response and avoiding a rotation collapse.

### 3. Magnetic Braking

Since the error field limit manifests itself by a loss of torque balance, the error field tolerance is determined by the torque that the non-axisymmetric perturbation exerts on the plasma.

#### 3.1. Rotation Evolution and Calculation of the Magnetic Braking Torque

In experiments with slowly increasing I-coil currents, the toroidal plasma rotation decreases across the entire profile, Fig. 5(a). In addition to a continuous rotation decrease, the rotation measurements taken at a fixed location also oscillate with the externally imposed rotation frequency  $f_{\text{ext}} = 10$  Hz. This oscillation is caused by a superposition of the externally applied rotating  $n = 1$  field with a residual (imperfectly corrected)  $n = 1$  intrinsic error field as well as convective transport with the kink-type displacement of the plasma response. The rotation profile during the slow braking phase does not show any evidence of a localized braking torque, Fig. 5(b). However, diffusive transport, the finite spatial resolution of the rotation measurements and the uncertainty of the measurements limit the detectability of a localized torque. Once the externally applied field exceeds the critical value (at  $t \approx 2140$  ms) the rotation collapse starts in the outer half of the plasma but quickly (typically in the order of 10 ms) propagates inwards, Fig. 5(a).

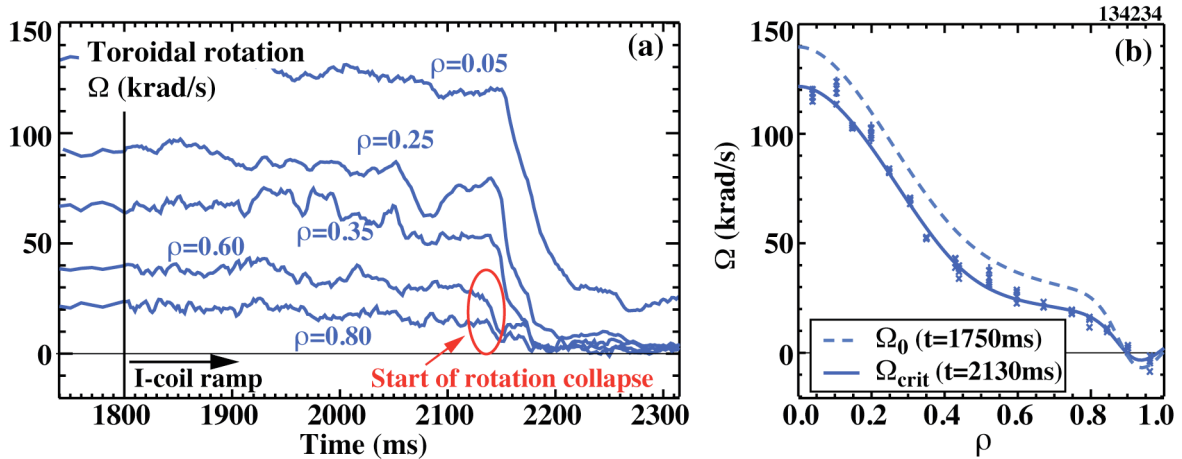


FIG. 5. Ramping up the I-coil current leads to a decay of the rotation across the entire profile (a). The rotation collapse starts in the outer half of the plasma but quickly affects the entire profile. Rotation measurements prior to the collapse (b) do not reveal any localized braking torque.

#### 3.2. Frequency Dependence of the Torque

The magnetic braking torque  $T_{\text{MB}}$  is obtained from the measured global rotation evolution,

$$T_{\text{MB}} = T_{\text{NBI}} - \frac{L}{\tau_{L,0}} - \frac{dL}{dt} . \quad (3)$$

The profiles for the transport calculation are averaged over the externally imposed oscillation period of  $T_{\text{ext}} = 100$  ms in order to suppress the non-axisymmetric effects on the

measurements discussed above, which are not part of the transport calculation. Since most magnetic torque models rely on a  $\delta j \times \delta B$  torque, where  $\delta j$  is induced through  $\delta B$ , it is tenable to assume that the magnetic torque has a  $\delta B^2$  dependence. Normalizing  $T_{MB}$  with  $\delta B^2$  then reveals the  $\Omega$  dependence, which is shown for  $\Omega$  at the  $q=2$  surface for several discharges in Fig. 6. While the discharge with the lowest rotation shows a torque that increases with decreasing  $\Omega$  the high rotation discharges show a torque that decreases with decreasing  $\Omega$ . The lowest torque is encountered when the rotation evaluated at the  $q=2$  surface is approximately 30 krad/s.

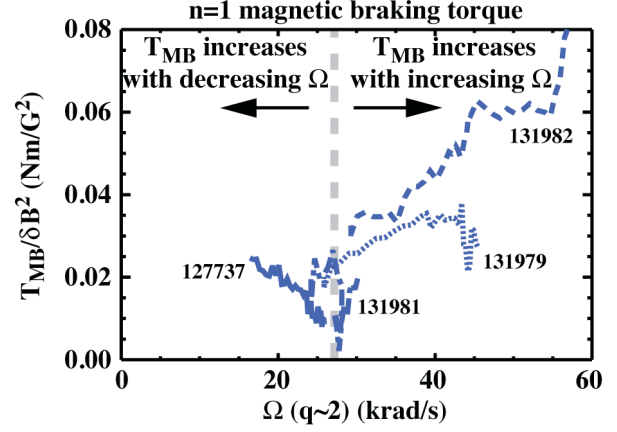


FIG. 6. The normalized magnetic braking torque  $T_{MB}/\delta B^2$  has a minimum at a rotation at  $q=2$  of  $\Omega(q=2) \approx 30$  krad/s.

### 3.3. Comparison of Resonant and Non-resonant Braking

While a magnetic torque that depends on  $\Omega^{-1}$  is usually associated with resonant braking and a torque that is proportional to  $\Omega$  with non-resonant braking [22], the actual  $\Omega$ -dependencies depend on the parameter regime (e.g., [6]). In this work a torque  $T_R = K_R \delta B_R^2 \Omega^{-1}$  is referred to as “resonant-like” and  $T_{NR} = K_{NR} \delta B_{NR}^2 \Omega$  as “non-resonant-like” torque. Adding a non-resonant-like to the typical resonant-like torque in the angular momentum evolution,

$$I \frac{d\Omega}{dt} = T_{in} - \frac{I\Omega}{\tau_{L,0}} - K_{NR} \delta B_{NR}^2 \Omega - K_R \delta B_R^2 \Omega^{-1} \quad (4)$$

results in a decrease of the rotation at the collapse from the characteristic  $\Omega_{crit} = \Omega_0/2$  of the resonant braking model (assuming that all other torques stay constant and that the viscous momentum transport is described by a momentum confinement time) to

$$\Omega_{crit} = \frac{1}{2} \frac{\tau_{L*}}{\tau_{L,0}} \Omega_0 \quad (5)$$

The effective momentum confinement time  $\tau_{L*} = (\tau_{L,0}^{-1} + I^{-1} K_{NR} \delta B_{NR}^2)^{-1}$  in Eq. (5) accounts for the confinement reduction caused by non-resonant-like magnetic braking. In experiments where  $T_{NBI}$  is kept constant the critical rotation  $\Omega_{crit}$  indeed indicates a deviation from the simple scaling with  $\Omega_{crit}$  at the highest initial rotation values  $\Omega_0$  falling below  $\Omega_0/2$ , Fig. 7. Moreover,  $\Omega_{crit}$  never exceeds 30 krad/s, which is close to the minimum of the torque, Fig. 6.

While a “non-resonant” torque cannot cause a bifurcation in the torque balance, it reduces the tolerable resonant field, which in the limit of large  $\delta B_{NR}$  becomes,

$$\delta B_{R,crit} = T_{in} \delta B_{NR}^{-1} (4K_R K_{NR})^{-1/2} \quad (6)$$

Since both,  $\delta B_R$  and  $\delta B_{NR}$  are proportional to  $I_{L,coil}$ , the linear dependence of  $I_{crit}$  on  $T_{in}$  motivated by Eq. (2) is reduced to  $I_{crit} \propto T_{in}^{0.5}$ . A fit of the measured values of  $I_{crit}$  to  $(T_0 + T_{NBI})^{0.5}$  results in an offset  $T_0 = 1.7$  Nm, Fig. 2, which is more compatible with an intrinsic rotation.

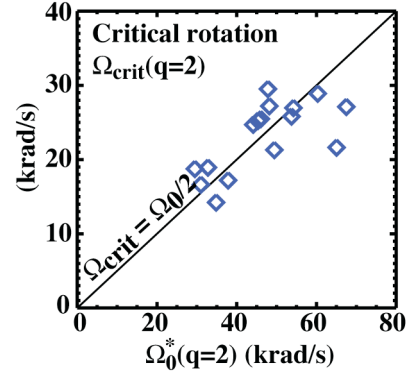


FIG. 7. The critical rotation  $\Omega_{crit}(q=2)$  never exceeds 30 krad/s. Discharges with an unperturbed rotation  $\Omega_0(q=2) > 60$  krad/s fall below the  $\Omega_{crit} = \Omega_0/2$  scaling.

#### 4. Conclusion and Summary

The limit to tolerable externally applied  $n = 1$  “error” fields in tokamak plasmas is caused by a bifurcation in the torque balance, which is followed by an error field-driven locked mode. The error field tolerance can be improved by increasing the torque input, e.g., with tangential NBI. The error field tolerance decreases with increasing  $\beta_N$ . This important  $\beta_N$  dependence was not previously appreciated, and was not included in the empirical scaling of the error field tolerance reported in the 1999 ITER Physics Basis [1]. The  $\beta_N$  dependence is explained by the dominant role of the plasma response to the externally applied field in the braking. Varying the poloidal spectrum of the externally applied field shows that the plasma response is caused by a resonant amplification of the stable  $n = 1$  kink mode. The increase of the amplification with  $\beta_N$  accelerates as the ideal MHD stable kink mode converts into a kinetically stabilized RWM above the no-wall stability limit. This has three important consequences for the (re-)evaluation of the error field tolerance in ITER: (1) Neglecting the  $\beta_N$  dependence in empirical scaling can lead to overly optimistic predictions for low torque, high  $\beta_N$  scenarios and, in particular, for advanced tokamak scenarios, which rely on operation in the wall-stabilized regime. (2) The error field tolerance has to be specified for the component that couples best to the kink mode, which has a lower pitch angle than the  $n = 1$  field that is resonant with rational surfaces inside the plasma and currently used for empirical scaling laws. (3) Correction coils even with a poorly matched magnetic field pattern should be effective in suppressing the plasma response and avoiding a rotation collapse. The measurable increase of the plasma response with  $\beta_N$  can then be exploited for “dynamic” correction of the field error using slow magnetic feedback.

#### Acknowledgments

The authors would like to thank Prof. A.H. Boozer and Drs. K.H. Burrell, A.J. Cole and S.A. Sabbagh for insightful discussions. This work was supported by the US Department of Energy under DE-FG02-89ER53297, DE-FC02-04ER54698 and DE-AC02-76CH03073.

#### References

- [1] ITER PHYSICS BASIS, Nucl. Fusion **39**, 2137 (1999).
- [2] HENDER, T.C., et al., Nucl. Fusion **32**, 2091 (1992).
- [3] La HAYE, R.J., HYATT, A.W. and SCOVILLE, J.T., Nucl. Fusion **32**, 2119 (1992).
- [4] GAROFALO, A.M., et al., Nucl. Fusion **47**, 1121 (2007).
- [5] GAROFALO, A.M., et al., Am. Phys. Soc. **52** 101 (2007).
- [6] FITZPATRICK, R., Nucl. Fusion **33**, 1049 (1993).
- [7] REIMERDES, H., et al., Plasma Phys. Control. Fusion **49**, B349 (2007).
- [8] OKABAYASHI, M., et al., this conference, EX/P9-5.
- [9] BUTTERY, R.J., et al., Phys. Plasmas **15**, 056115 (2007).
- [10] BUTTERY, R.J., et al., this conference, IT/P6-8.
- [11] SOLOMON, W.M., et al., this conference EX/3-4.
- [12] GAROFALO, A.M., et al., Phys. Plasmas **9**, 1997 (2002).
- [13] BOOZER, A.H., Phys. Rev. Lett. **86**, 5059 (2001).
- [14] LIU, Y.Q., et al., Phys. Plasmas **7**, 3681 (2000).
- [15] HU, B., BETTI, R., Phys. Rev. Lett. **93**, 105002 (2004).
- [16] BONDESON, A., CHU, M.S., Phys. Plasmas **3**, 3013 (1996).
- [17] BONDESON, A., WARD, D.J., Phys. Rev. Lett. **72**, 2709 (1994).
- [18] PARK, J.-K., SCHAFFER, M.J., MENARD, J.M., BOOZER, A.H., Phys. Rev. Lett. **99**, 195003 (2007).
- [19] PARK, J.-K., BOOZER, A.H., GLASSER, A.H., Phys. Plasmas **14**, 052110 (2007).
- [20] REIMERDES, H., et al., Phys. Rev. Lett. **93**, 135002 (2004).
- [21] LIU, Y., et al., Phys. Plasmas **13**, 056120 (2006).
- [22] SHAIN, K.C., Phys. Plasmas **10**, 1443 (2003).